

Exploration of Lower Cretaceous sands in the Leland Area, Alberta, using seismically derived rock properties

After describing the processing sequence necessary, Carmen C. Dumitrescu,^{1*} Fred Mayer² and Rodney Couzens¹ present a study based on Canadian data in improving the resolution of different seismic attributes obtained from deterministic inversion using neural network analysis.

The Leland area (Figure 1a) is located in the Western Canadian Foreland Basin in Alberta, Canada. The Lower Cretaceous Cadomin Formation (Figure 1b) consists of conglomeratic sands deposited as a series of alluvial fans shed off the incipient mountain ranges located to the south west and reworked by a braided stream system (Figure 2). The Cadomin Formation is underlain by tight marine sands and shales of the Jurassic Nikinassin and Fernie Formations, and overlain by the fluvial sands and coals of the Gething Formation. The Leland area is located within, but close to the edge of the Deep Basin hydrodynamic trap region where gas is trapped in porous sands by updip water due to relative permeability changes. Typical reservoir porosities are in the 6–12% range, with thicknesses of 5–10 m. The Leland field produced about 80 MMcf/day, in 2006.

The Leland area was recently explored for a deeper Devonian target. This resulted in a legacy of good quality 3D seismic data coverage and a number of wells which penetrated the Cadomin Formation. The Cadomin is a difficult sand to explore using conventional interpretation techniques. Forward modelling of porosity changes in the Cadomin does not yield a consistent porosity signature in the seismic data and zero-offset synthetics often do not tie the seismic character properly. The Cadomin does not have a consistent seismic expression, sometimes appearing as a peak, a trough, or a zero-crossing.

It is well known and accepted by the industry that inversion is a necessary step in imaging and interpreting the reservoir and there is a continuous struggle to improve the resolution and accuracy of the inverted volume. In this project we used probabilistic neural network analysis (PNN) for estimating new seismic volumes by integrating well information and existing seismic volumes (e.g., deterministic inversion results). The seismic volumes were processed through a model-based inversion algorithm to produce P-impedance, S-impedance, and density volumes. These volumes were used as attributes in the neural network analysis. The density from inversion was remarkably consistent with a well based porosity-thickness (Phi-h) map (Figure 3). The Deep Basin trap line separates the

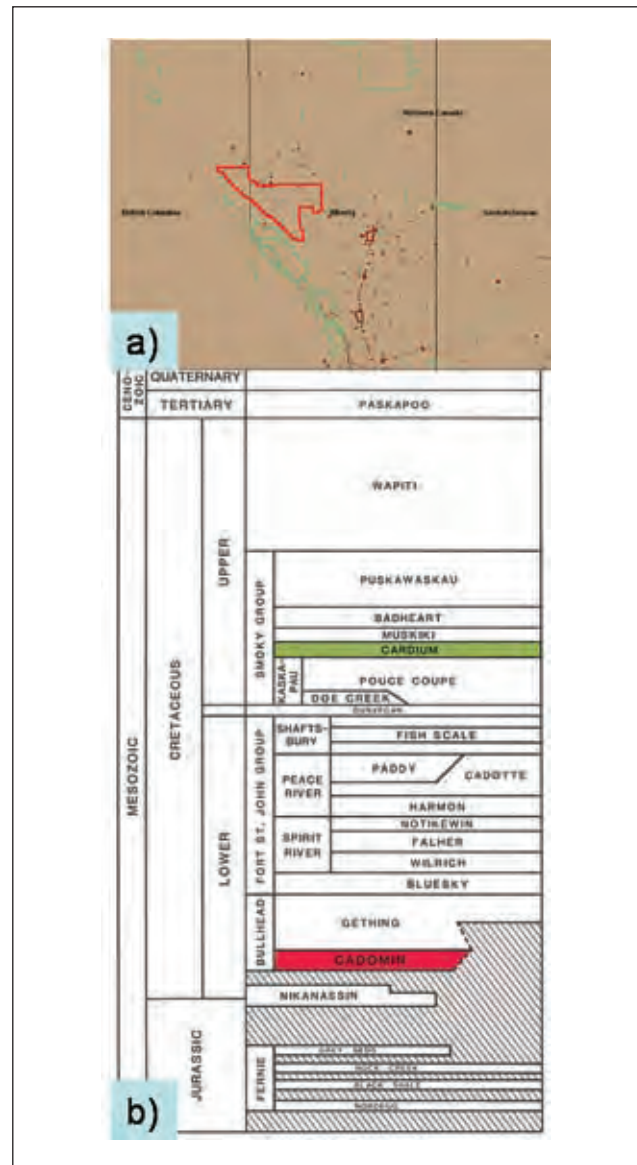


Figure 1 (a) Location of the Leland Area in Alberta, Canada; (b) Table of Stratigraphic names in the Deep Basin Mesozoic section (Gies, 1984).

¹ Sensor Geophysical.

² Devon Canada Corporation.

* Corresponding author, E-mail: carmen_dumitrescu@sensorgeo.com

Reservoir Geoscience and Engineering

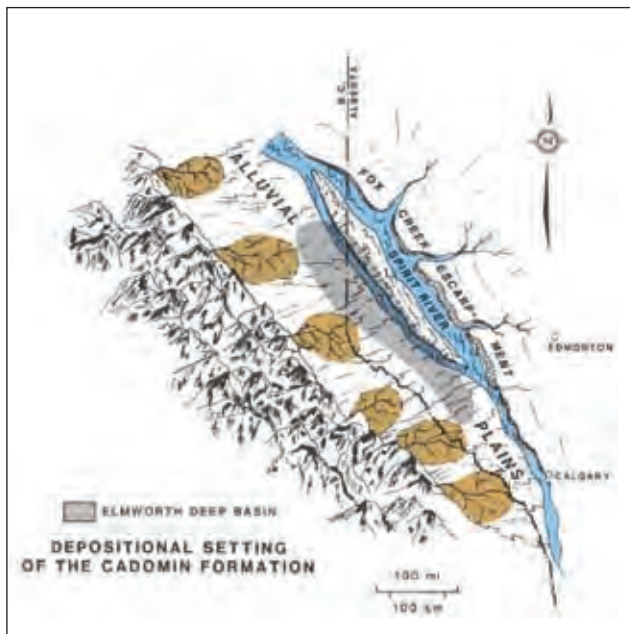


Figure 2 Cadomin Formation depositional environments (Gies, 1984).

conventional reservoir domain from the deep basin reservoir where porous sand is always gas sand (there is no water).

Method

(1) Basic processing of the seismic data

In general, the prestack application of data driven time-variant trace by trace spectral shaping and amplitude scaling and the deferral of some noise attenuation processes until after common-midpoint stacking tends to produce the most interpretable stacked volumes. However, to obtain the best gathers for AVO analysis all spectral shaping and scaling corrections should instead be model-driven or derived

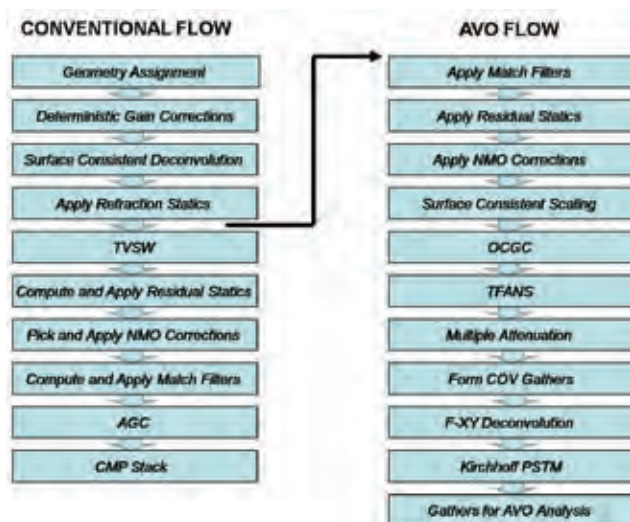


Figure 4 Processing workflow for time domain seismic data.

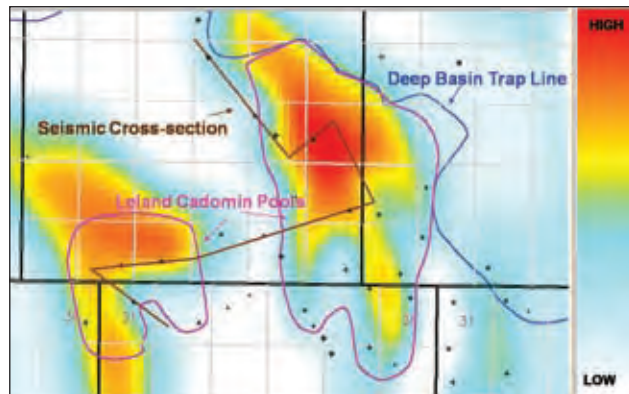


Figure 3 Porosity-thickness (Phi-h) map of the Cadomin Formation area including the contours of two of the Leland Cadomin Pools (pink), the seismic cross-section used for the seismic examples (brown), and the Deep Basin trap line (blue).

from global or surface consistent analyses, and noise that is either adequately attenuated simply by CMP stacking or best addressed poststack may need instead to be attenuated prestack. Consequently, two different processing sequences must normally be executed when gathers are required for AVO analysis. The first to be run may be thought of as the ‘conventional’ processing flow, from which optimum statics and velocity estimates are obtained, along with an optimum stacked volume. The second flow to be run may be thought of as the ‘AVO compliant’ processing flow. It typically reuses the statics and velocities obtained from the first flow, but usually works harder to attenuate both ambient and source generated noise, including multiples, contains prestack imaging steps, and at all times tries to preserve valid relative amplitude variations. Both flows may also strive to preserve greater incident angles than usual by attempting, for example, to accurately correct for non-hyperbolic long offset NMO.

The processing of the 3D seismic data used in this study adhered to this typical methodology. Merging of the six different 3D surveys making up the full dataset examined here was done in the conventional processing flow. These individual surveys, recorded between 1996 and 2003, were all obtained with a dynamite source, but with dissimilar hole depths, charge sizes, and acquisition geometries. Determination of the refraction and residual statics, stacking velocities, and match filters required to optimize the CMP stack of this combination of surveys fell under the purview of the conventional processing flow which, after surface consistent deconvolution, employed passes of data driven trace by trace time-variant spectral whitening (TVSW) and amplitude scaling (AGC) to assist with the effort.

After several iterations in the conventional flow to optimize statics and velocity estimates, the AVO compliant flow commenced, picking up data from the conventional flow after surface consistent deconvolution, but replacing the

Reservoir Geoscience and Engineering

TVSW step with a common source gather time-frequency analysis (TFANS) to identify and suppress anomalously high amplitudes present within restricted time and frequency ranges, and replacing the AGC step with iterative passes of surface consistent scaling and global time-variant offset consistent gain corrections (OCGC). Radon filtering was also used in this flow to attenuate short period multiples present in the zone of interest. Common offset vector gathers (COVs) were formed after these noise attenuation and scaling steps, and subsequent to applying statics and partial NMO corrections. F-xy prediction filtering was used to clean up these COV gathers, which were then input to a migration velocity analysis process and then ultimately to the Kirchhoff prestack time migration (PSTM) pass which output gathers ready for the subsequent AVO analysis.

(2) Petrophysical analysis and forward modelling

Petrophysical analysis was performed on all raw log data in order to provide a trustworthy set of logs for inversions and multi-attribute analysis. The analysis included edits and corrections for poor-quality logs (mainly the density). Missing curves (e.g., shear sonic and density) were estimated using either the specific mud-rock line for the zone of interest or a neural network analysis that allows us to estimate missing logs from existing logs. For all the dipole wells, Lambda-Rho (LR), Mu-Rho (MR), and Lambda-Rho over Mu-Rho (LR/MR) logs were calculated and analyzed for lithology identification, yielding the main conclusions: (1) porous sands have low LR, high MR, and low LR/MR ratio; (2) coals have low LR, low MR, and high LR/MR ratio (Figure 5).

Crossplots of several properties over the target interval (Figure 6) were used (i) in identifying lithology (Figure 6a), (ii) in finding the V_s - V_p relationship (Figure 6b) that was used in the AVO analysis, and (iii) in finding the linear relationship in the logarithmic domain between P-impedance (Z_p),

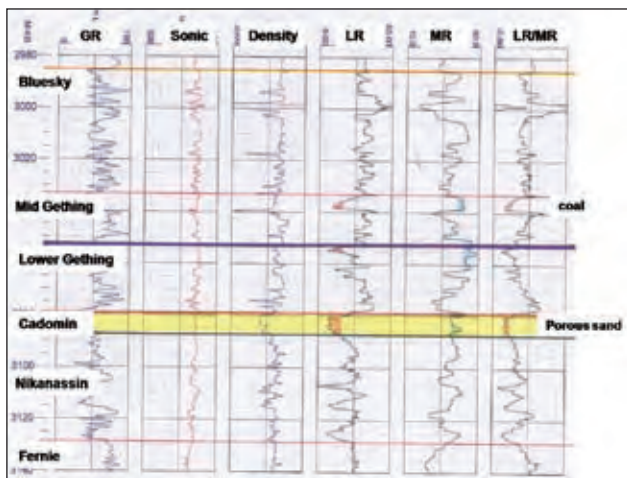


Figure 5 A typical set of raw logs for the Lower Cretaceous group, include gamma ray (GR), sonic and density. Estimated logs such as LR, MR, and LR/MR are used to differentiate between coal and porous sand.

S-impedance (Z_s), and Density (D_n) (Figure 6c). These latest relationships were used in the prestack inversion. Figure 6a shows crossplots of Lambda-Rho and Mu-Rho coloured by gamma-ray and density. Based on the lowest density values we defined the coals and, based on the gamma-ray values, we separated the gas sand (low GR) from shale (high GR).

Conventional forward modeling (Figure 7) and a seismic cross-section (Figure 8) through the same wells yields no consistent porosity signature at the Cadomin Formation.

(3) Special processing workflow

Step 1: AVO analysis

Preparation for AVO analysis includes: (i) creating offset synthetics (Figure 9); (ii) analyzing zero-offset synthetic ties to P-wave reflectivity seismic data to establish proper phase rotation; (iii) applying the identified phase rotation to the AVO gathers to produce zero phase P and S reflectivity sections; (iv) mapping the base of coal to Cadomin Formation isochron to create a synthetic Cadomin pick to be used for attribute windows (Figure 10).

Based on the offset synthetics the Cadomin Formation porosity exhibits a type II AVO anomaly, the Gething Formation channel is a prominent peak at far offsets and a varying 3D offset mix complicates the stacked data. Variation of offset mix in the 3D dataset causes a seismic expression change, even if the reservoir itself remains unchanged.

The eventual method used to find the Cadomin level was to map out an isochron from a consistent marker located above the formation. The map was created by contouring and gridding isochron values measured from good well ties which had been squeezed/stretched to fit. The grid was converted to an isochron map which was added to the overlying reflector to give a pseudo Cadomin time pick.

AVO analysis was performed using Fatti's equation and a velocity model derived from the correlated wells and seismic data. Attributes resulting from this analysis include P- and S-wave impedance reflectivities and Fluid Factor (Figure 11). The fluid factor attribute was measured in windows above and below the Cadomin for mapping.

Step 2: Deterministic inversion

Prestack inversion was performed on prestack time migrated gathers to derive P-impedance, S-impedance, density, and V_p/V_s followed by the calculation of rock properties (Goodway et al., 1997) such as rigidity (Mu-Rho) and incompressibility (Lambda-Rho). Prestack inversion uses the fact that the basic variables P- and S-impedance and density are coupled by two linear relationships which should hold for the background 'wet' trend.

All these inversion attributes were mapped in appropriate windows and compared with the logs but the results are too biased, especially in the vicinity of the coals.

Reservoir Geoscience and Engineering

Step 3: Neural network analysis for P-impedance, S-impedance, and density.

By training a neural network with a statistically representative population of the targeted log responses (P-impedance, S-impedance, or density) and several seismic attribute volumes available at each well, firstly, a linear multi-attribute transform was computed to produce P-impedance, S-impedance, and density volumes. Then, the linear multi-attribute relation was used in the estimation of the

non-linear relation from neural network computation. A complete description of the neural network usage for increasing the resolution of inversion attributes is provided by Dumitrescu and Lines (2009).

The P- and S-impedance results from neural network analysis were used in the calculation of Lambda-Rho and Mu-Rho attributes. The new Lambda-Rho and Mu-Rho seismic volumes (i) show better resolution, (ii) ties better to well data, and (iii) eliminate the spurious anomalies.

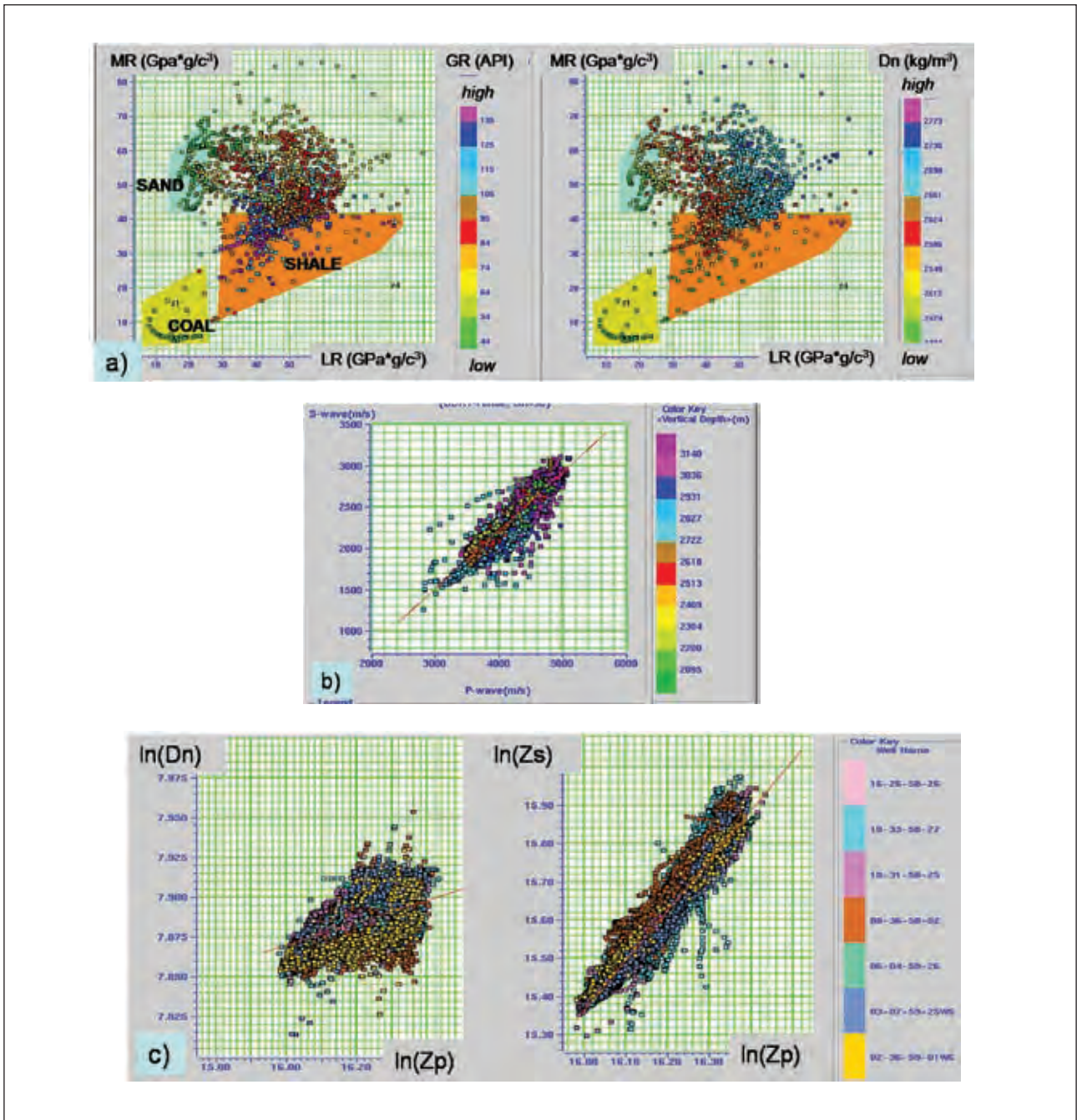


Figure 6 Crossplot of (a) Mu-Rho versus Lambda-Rho; (b) Vs versus Vp for Lower Cretaceous and (c) ln(Dn) versus ln(Zp) and ln(Zs) versus ln(Zp).

Reservoir Geoscience and Engineering

Special attention was paid to the generation of the density volume, because all the logs indicate big variations in the density associated with porous sands, coals, and shales in contrast to the minimal changes in the sonic logs. Depth of formation precludes the use of three-term AVO for density, so neural network density inversion was performed in an effort to account for non-linear relationships between

logs and seismic after first testing the linear multi-attribute method alone.

Case study

Deterministic inversion and neural network analysis applied to the 3D seismic volume in the Leland area, a Cadomin gas reservoir in the Deep Basin, greatly help to define the gas sands and to better differentiate between gas sands and coals in the overlying Lower Gething Formation.

In this paper we show how neural network analysis for estimating P-impedance and density volumes improved the results from deterministic inversion. The logs obtained from petrophysical analysis were candidates for the training analysis, but only the well ties with good correlations (38 out of 47 wells) were used in the neural network analysis. Validation analysis was used to ensure that the neural network (and the multi-attribute) analysis was not over predicted (Hampson et al., 2001).

Neural network analysis for P-impedance used the calculated P-impedance logs as target logs and the migrated seismic volume and the P-impedance volume (from model based inversion) as external attributes. The correlation was 86% on the validation of the neural network analysis. The PNN results were applied to the seismic volume from 100 ms above Mannville Formation to 30 ms below Cadomin Formation.

P-impedance results from model based inversion (Figure 12a) are compared with the P-impedance results



Figure 7 Conventional forward modelling yields no consistent porosity signature.

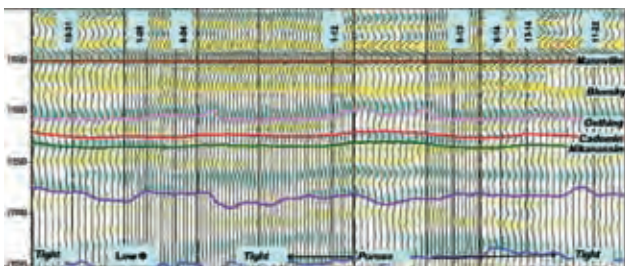


Figure 8 Cross-section through some of the wells on the 3D seismic data.

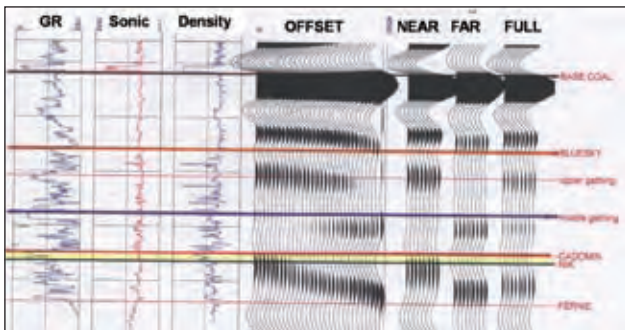


Figure 9 Cadomin Formation offset synthetic.

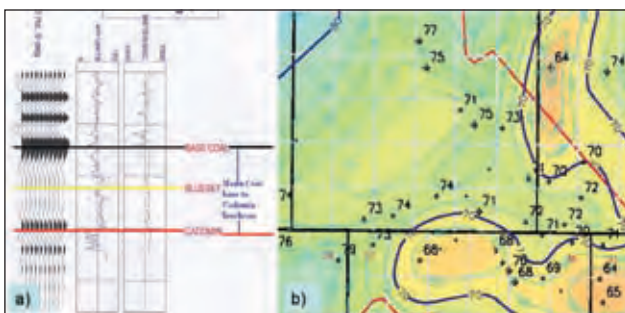


Figure 10 Mannville Formation Coal Base to Cadomin Formation Isochron; (a) isochron measured from synthetic; (b) isochron values at wells contoured, gridded and converted to horizon.

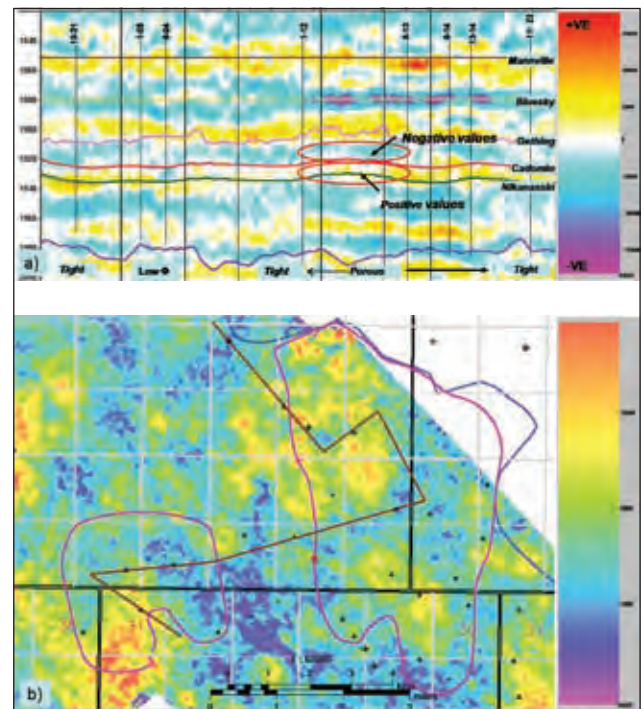


Figure 11 (a) Fluid Factor section; (b) Fluid Factor Attribute – sum of absolute values above and below Cadomin Formation pick.

Reservoir Geoscience and Engineering

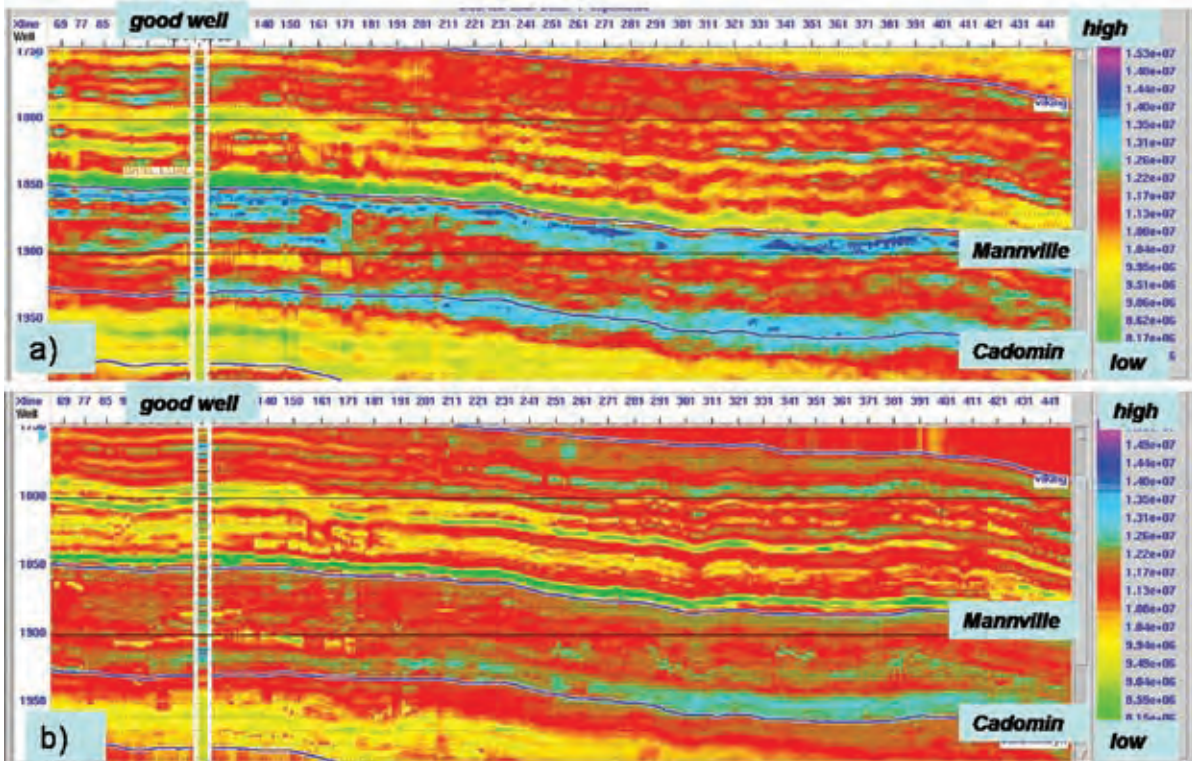


Figure 12 P-impedance results from (a) model based inversion and (b) neural network analysis. Inserted in colour is the P-impedance log that correlates much better with neural network results.

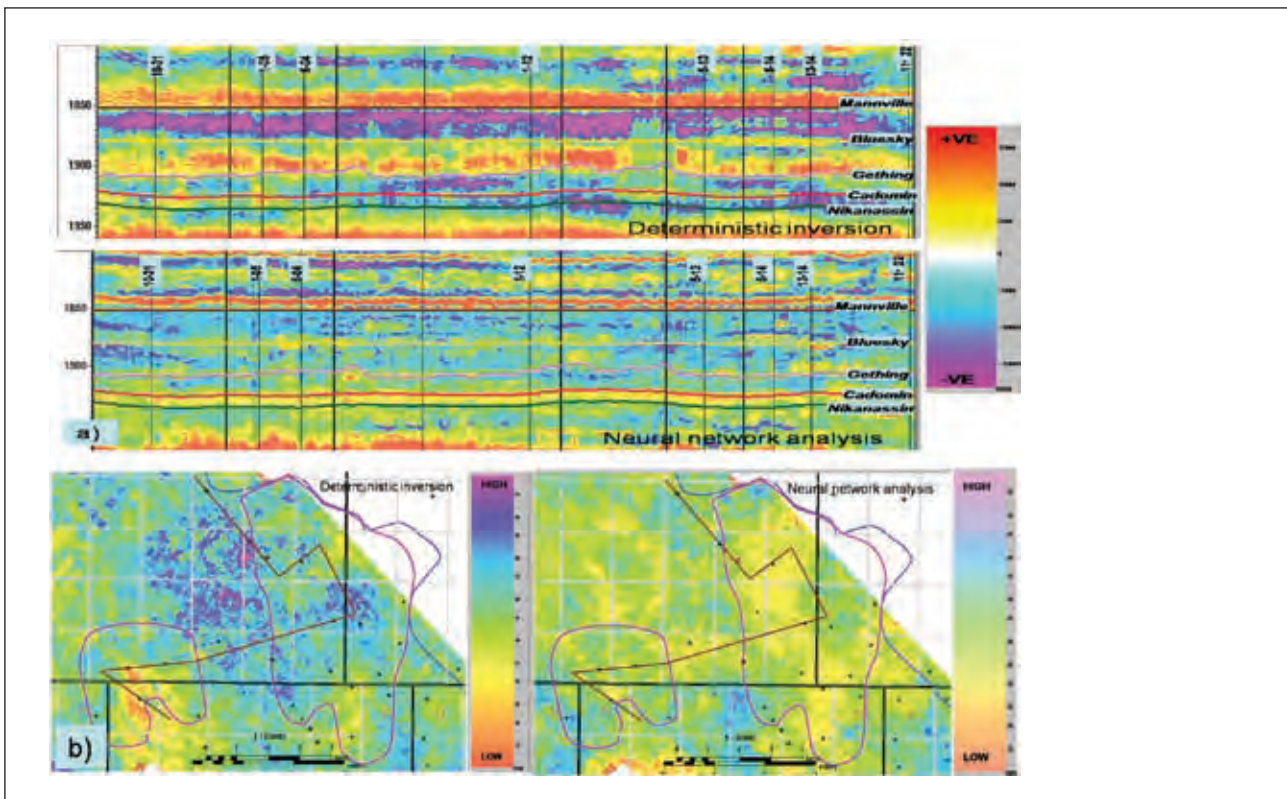


Figure 13 Comparison of deterministic and neural network Lambda-Rho displayed on (a) seismic cross-section; (b) average value in Cadomin Formation window.

Reservoir Geoscience and Engineering

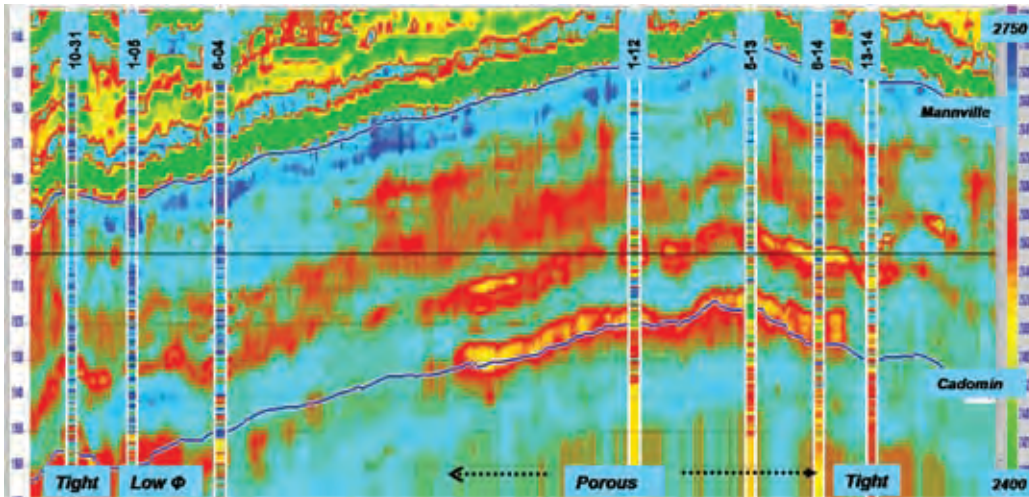


Figure 14 Density results from neural network analysis. Inserted in colour is the density log which correlates much better with neural network results.

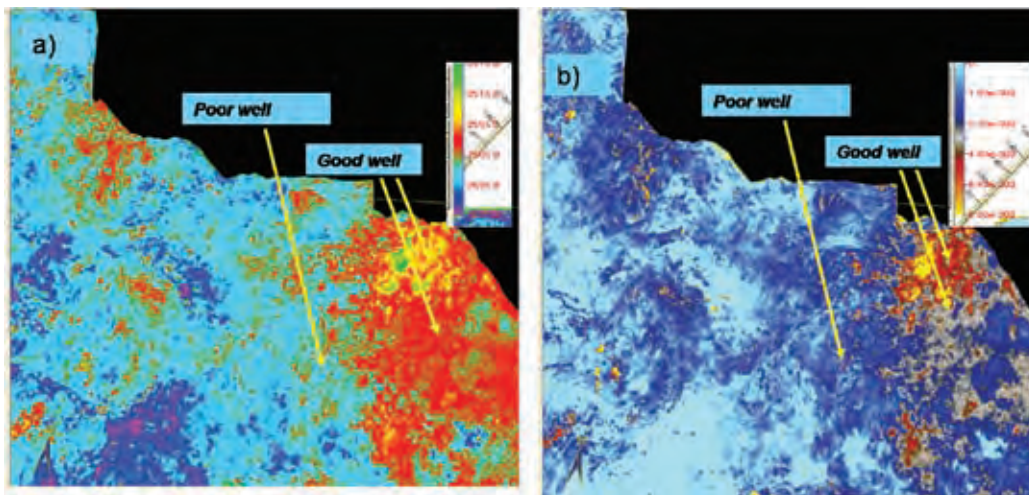


Figure 15 Horizon slice at Cadomin Formation+6 ms of the (a) density results from neural network analysis and (b) porosity results from the inverted density response using a standard linear-density relationship. Note the distinct separation of sand from silt and shale.

from neural network analysis (Figure 12b) on the seismic cross-section presented in Figure 3. Inserted in colour in Figure 12 are the P-impedance logs from several wells. P-impedance results from neural network analysis show a better correlation with the log and offer a better definition of the Mannville Formation coals.

Refining the P-impedance results from deterministic inversion with neural network analysis proved to be a very useful step also in improving the rock properties results such as rigidity and incompressibility presented in Figure 13.

Density is a useful property in differentiating porosity within sands. A density volume from prestack inversion is just a first approximation of the density volume. Since we have only up to 29° on the angle gathers, the density results are based on the linear relationship in the logarithmic domain derived between P-impedance and density on the petrophysical analysis (see Figure 6c). Neural network analy-

sis for density used density logs, obtained from petrophysical analysis, as target logs and six seismic volumes available from AVO and inversion. Using the ranking process available within the software and after checking the errors, we selected the following attributes for training the network and to estimate the density:

- P-impedance
- S-impedance
- Amplitude envelope of P-wave reflectivity trace
- Integrated absolute amplitude of S-wave reflectivity trace
- Filter 35/40 - 45/50 of the migrated stack
- Integration of the S-wave reflectivity trace
- Instantaneous frequency of the S-wave reflectivity trace

Figure 14 presents density cross-section results from neural network analysis. By this method, density can be estimated from data which does not have enough offsets for three-term

Reservoir Geoscience and Engineering

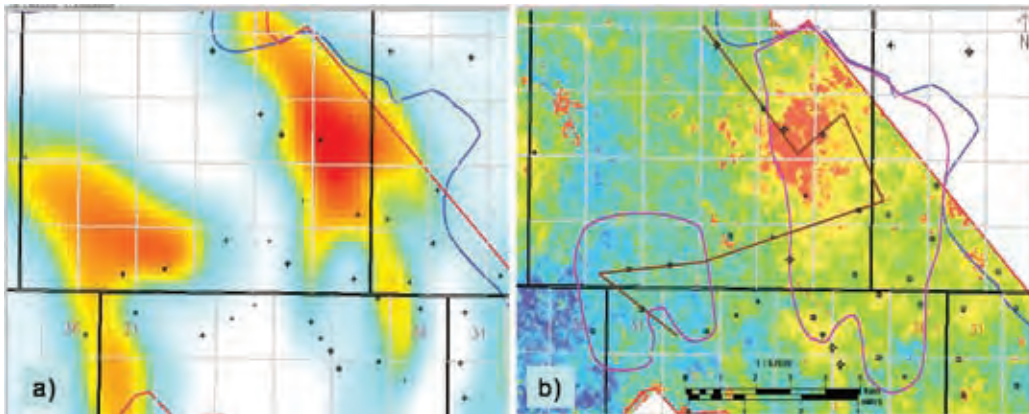


Figure 16 Comparison of Cadomin Formation Phi-h from well data to average density in Cadomin window.

AVO. The density results from the neural network analysis correlate with wells available on the 3D seismic survey, even if the wells have not been used for the analysis.

The density volume from neural network analysis (Figure 15a) was used to estimate the porosity using a standard linear-density relationship (Figure 15b). The horizon slice at Cadomin Formation+6 ms on the computed porosity volume shows good definition of the reservoir. It is clear that the estimated seismic volumes from neural network analysis provide meaningful information in identifying the gas sands.

Finally, we compared the original Cadomin Formation Phi-h map with the average density in Cadomin window and found out that for the East-Leland pool the two maps are very similar, but for the western pool there are differences. Those differences can be explained because the porosity is very poor but the Cadomin Formation is thicker.

Conclusions

We have presented a case study for improving the resolution of different seismic attributes (e.g., P-impedance and density) obtained from deterministic inversion by using neural network analysis.

The derived neural network results show strong correlation with the target logs, both at training well locations and for the rest of the wells suggesting that rock properties can be accurately estimated with neural network analysis when deterministic inversion results are used as external

attributes in training the network. Neural network analysis for rock properties (rigidity and incompressibility) can see the thin Gething Formation channels and identify the porosity changes in the Cadomin Formation. Density estimation allows direct comparison of seismic data to well based Phi-h (porosity-thickness) maps.

References

- Dumitrescu, C.C. and Lines, L., [2009] Characterization of heavy oil reservoir using Vp/Vs ratio and neural network analysis. In: Chopra, S., Lines, L.R., Schmitt, D. and Batzle, M. L. (Eds) *Heavy Oils – Reservoir Characterization and Production Monitoring*. SEG in press.
- Gies, R. M. [1984] Case history for a major Alberta Deep Basin gas trap: The Cadomin Formation. In: Masters, J.A. (Ed) *Case Study of a Deep Basin gas field*. AAPG, Tulsa, Oklahoma, p. 316
- Goodway, W., Chen, T. and Downton, J. [1997] Improved AVO fluid detection and lithology discrimination using Lamé petrophysical parameters; 'Lambda-Rho', 'Mu-Rho' and 'Lambda/Mu stack', from P and S inversions. *CSEG Annual Meeting*, Abstracts, 141-151
- Hampson, D., Schuelke, J. S. and Quirein, J.A. [2001] Use of multi-attribute transforms to predict log properties from seismic data. *Geophysics*, 66, 220-23.

Acknowledgements

The authors thank Sensor Geophysical, Devon Canada Corporation, Devon's partners, and Time Seismic.

Visit www.eage.org/jobs

Looking for a new Challenge?
Surf to our website and have a
look at the latest Job openings!